Research Square

Preprints are preliminary reports that have not undergone peer review.
They should not be considered conclusive, used to inform clinical practice,
or referenced by the media as validated information.

Network-Dependent and Amyloid-Dominant Pathways Link Early Regional Amyloid to Cognition Before Global Amyloid Positivity

Chuyao Yan
Nanjing Normal University
Marcel Daamen
University of Bonn
Xiaochen Hu
Shanghai Jiao Tong University School of Medicine
Henning Boecker
University of Bonn
Hao Wang
Hainan University
Ying Han
Xuan Wu Hospital of the Capital Medical University
Xueyan Jiang
xjiang@nju.edu.cn

Nanjing University

Research Article

Keywords: Amyloid-β, Global amyloid-negative, Network-dependent

Posted Date: November 3rd, 2026

DOI: https://doi.org/10.21203/rs.3.rs-11565606/v1

License: This work is licensed under a Creative Commons Attribution 4.0 International License. Read Full License

Additional Declarations: No competing interests reported.

Abstract

Background and Objectives

: Global amyloid-β (Aβ) positivity is commonly defined by thresholds intended to identify widespread cortical pathology, yet such thresholds may obscure biologically meaningful regional Aβ accumulation before individuals cross the threshold for global positivity. Here, we asked whether early regional Aβ deposition in globally Aβ-negative (gAβ−) individuals is cognitively consequential, and whether its impact depends on the brain's network architecture.

Methods

Using multimodal imaging and cognitive data from the Sino Longitudinal Study on Cognitive Decline (SILCODE), we examined associations between regional Aβ burden and cognition as a function of structural and functional network topology, with longitudinal analyses within SILCODE and validation of cognitive and amyloid trajectories in the independent Harvard Aging Brain Study (HABS).

Results

In gAβ − individuals, regional Aβ exhibited marked heterogeneity in its cognitive relevance. Precuneus Aβ showed a topology-independent association with cognition, defining an amyloid-dominant pathway. In contrast, Aβ in several network-integrated regions including the anterior cingulate, inferior frontal gyrus pars triangularis, parahippocampal, supramarginal, postcentral, superior temporal, and middle temporal gyri was cognitively relevant primarily in relation to structural network centrality, indicating a network-dependent pathway. Longitudinally, the anterior cingulate Aβ × degree interaction predicted subsequent cognitive trajectories in SILCODE. Consistent with these findings, regional Aβ in several topology-dependent regions predicted cognitive decline over 3- and 8-year follow-up in HABS, whereas precuneus Aβ consistently predicted subsequent global amyloid progression.

Conclusions

Together, these findings reveal that global Aβ negativity does not necessarily signify the absence of cognitively relevant amyloid pathology. Instead, early regional Aβ may engage distinct pathways before global amyloid positivity: a precuneus-centered pathway linked to subsequent amyloid propagation and a network-dependent pathway through which local topology shapes its cognitive relevance. These results highlight the importance of regional and network-level organization for detecting and interpreting amyloid pathology below conventional global thresholds.

Introduction

The globally amyloid-negative (gAβ−) state, defined by amyloid PET, represents a critical yet poorly characterized window in the Alzheimer's disease (AD) continuum. Anti-amyloid therapies are thought to be most effective when initiated at the earliest stages of Aβ accumulation, before overt neurodegeneration has occurred[1,2], a pattern consistent with clinical trial data showing greater treatment benefit in earlier-stage, lower-pathology participants[3,4]. Yet current biomarker frameworks define preclinical AD primarily through global Aβ positivity (gAβ+)[5,6], a threshold derived to discriminate clinically or pathologically advanced cases from healthy controls rather than to capture the earliest emergence of amyloid pathology[7,8]. Consistent with this limitation, individuals classified as globally amyloid-negative are not biologically homogeneous: region-based staging approaches have revealed substantial heterogeneity in focal Aβ accumulation within this nominally negative population, heterogeneity that binary global classification overlooks entirely[9,10]. The gAβ − state therefore constitutes a window in which meaningful regional variation in amyloid burden already exists, but remains obscured by reliance on a single global metric.

This regional variation is not random: amyloid accumulation follows a relatively consistent spatial staging sequence, with certain association cortices affected earlier and more consistently than others across the AD continuum[11–13]. Because this staging order reflects how early a given region is affected, regional Aβ burden may carry more fine-grained disease-relevant information than a single global average, which collapses this ordered spatial pattern into one undifferentiated value. This possibility is supported by evidence that regional Aβ burden, particularly within the precuneus and posterior default mode network, relates to cognitive performance and predicts subsequent cognitive decline and pathological progression even before individuals reach global amyloid positivity[14,15], in contrast to the global Aβ and cognition literature, where associations in cognitively unimpaired individuals have generally been weak[16]. Yet, regional Aβ burden alone does not explain why amyloid deposition in some regions is more cognitively consequential than in others.

The clinical impact of localized Aβ may be fundamentally governed by the brain's systemic architecture rather than local burden alone. From a graph-theoretical perspective, the human connectome is organized around high-degree hubs that support efficient information integration across distributed neural systems[17,18]. While this topology enables efficient communication, it also renders hubs disproportionately vulnerable to pathological perturbations, as damage to these regions can propagate broadly across large-scale networks[19]. Consistent with this vulnerability, prior neuroimaging studies have identified hubs as primary targets of disruption in early AD[20,21], and recent evidence further suggests that Aβ deposition within these regions drives system-level network dysregulation even at the earliest stages of accumulation[22,23]. However, prior work in this area has primarily characterized how network architecture or activity shapes the spatial distribution of Aβ pathology[24], how network properties are altered once pathology has accumulated[25,26], or how connectome information can be incorporated into a composite pathology metric to improve overall predictive accuracy[27]. What these approaches have not addressed is whether, and at what point in the pathological process, a region's topological role changes the cognitive consequences of its amyloid burden.

To address this question, the present study leveraged two independent, longitudinal, globally amyloid-negative cohorts spanning the preclinical Alzheimer's disease continuum, the Sino Longitudinal Study on Cognitive Decline (SILCODE), and the Harvard Aging Brain Study (HABS). Using baseline PET, resting-state functional MRI, and diffusion tensor imaging data from SILCODE, we examined whether regional Aβ burden is associated with cognition, assessed by the Preclinical Alzheimer's Cognitive Composite (PACC), independently or through interaction with structural and functional network topology, and whether such associations differ between structural and functional network modalities. We then assessed whether these baseline associations extended to longitudinal cognitive change over a follow-up period ranging from 6 to 110 months. We further tested whether baseline regional Aβ burden in the implicated regions predicted subsequent cognitive decline and global amyloid accumulation in the independent longitudinal HABS cohort, capturing short-term change over 3-years, as well as longer-term trajectories over up to 8 years. Together, this multi-cohort design, spanning both cross-sectional and longitudinal analyses, provides a rigorous test of whether, and how, brain network architecture modulates the cognitive consequences of amyloid pathology before it becomes globally detectable.

Materials and methods

The overall methodological framework, including data processing and analytical modules, is illustrated in Fig. 1.

Cohorts and Participants

Participants were drawn from two independent cohorts: the Sino Longitudinal Study on Cognitive Decline (SILCODE)[28], and the Harvard Aging Brain Study (HABS)[29]. Cognitively normal (CN) or subjective cognitive decline (SCD) individuals with MMSE ≥ 25, CDR = 0, and available amyloid PET imaging from both cohorts were selected for the present analyses. Cohort-specific inclusion and exclusion criteria are provided in the *Supplementary Methods*.

The SILCODE cohort (N = 85) was used for baseline regional and network-informed analyses. The HABS cohort (N = 249 with 3-year follow-up, N = 102 with 8-year follow-up) were used for longitudinal prediction analyses of cognitive decline, global Aβ accumulation, and conversion to global Aβ positivity.

Both cohorts received approval from the institutional review boards of all participating centers, and written informed consent was obtained from all participants or their authorized representatives (clinical registration numbers: NCT0337074 and NCT00106899). Table 1 summarizes demographic and clinical characteristics for each cohort.

Table 1
Demographic and clinical characteristics for global amyloid negative (gAβ-) participants within each cohort.

	Cohorts		
	SILCODE	**HABS(0-3years)**	**HABS(0-8years)**
Age	65.88 ± 4.56	69.90 ± 8.62	71.62 ± 5.76
Sex (M/F)	23/50	50/107	29/43
Years of education	12.47 ± 2.97	15.95 ± 2.88	15.88 ± 2.96
APOE ε4 carriers, N (%)	24 (32.9%)	25(15.9%)	9 (12.5%)
Global SUVR	0.918 ± 0.102	1.101 ± 0.099	1.101 ± 0.099
PACC baseline	0.00 ±0.589	0.00 ± 0.650	0.00 ± 0.831
Follow-up (time/point)	1–8 times (6-110 months)	2 times 3 years	2 times 8years
Global SUVR at follow-up	/	1.179 ± 0.119	1.237 ± 0.158
PACC at follow-up	-0.240 ± 0.902	0.149 ± 0.886	-0.180 ± 1.072

Note: SUVR, standardized uptake value ratio; M, male; F, female; PACC, Preclinical Alzheimer's Cognitive Composite. Date was presented as mean±std.

Cognitive Performance

Cognitive performance was assessed using the Preclinical Alzheimer's Cognitive Composite (PACC), which is sensitive to Aβ-related decline in preclinical AD[30]. PACC scores were computed as the mean of standardized z-scores derived from multiple cognitive tests within each cohort, and the longitudinal PACC were normalized using the baseline data. For SILCODE, PACC included Chinese Mini-Mental Status, CMMS[31], Auditory Verbal Learning Test (AVLT), Animal Fluency Test (AFT), and Shape Trail Test Parts A and B (STTA–B). For HABS, it included MMSE, LMDR, Digit-Symbol Substitution, FCSRT (cued and free recall), and Category Fluency. To ensure cohort-specific normative calibration, z-scoring for each test was performed relative to the global amyloid-negative

subgroup within each respective cohort. Despite differences in test composition, baseline PACC distributions were comparable across cohorts, enabling harmonized assessment of preclinical cognitive function. Further details are provided in the *Supplementary Methods*.

PET Acquisition and Processing

Amyloid PET acquisition followed standardized cohort-specific protocols. SILCODE[28] used [^{18}F]-Florbetapir, while HABS[29] used [^{11}C]-PiB. All PET data underwent reconstruction, head-motion correction, co-registration to individual T1 images, and spatial normalization to MNI space. Detailed acquisition and processing parameters are described in the *Supplementary Methods*.

Global Amyloid Burden and Positivity

Global amyloid burden was quantified by averaging standardized uptake value ratios (SUVRs) across six harmonized cortical macro-regions: frontal, temporal, parietal, anterior cingulate, posterior cingulate, and precuneus[32]. Cohort-specific cerebellar gray-matter reference regions and established SUVR thresholds were used to classify global Aβ positivity (SUVR > 1.20 for SILCODE[23,33]; SUVR > 1.28 for HABS[29]). To capture the earliest stages of amyloid accumulation, only participants classified as globally Aβ- were included in regional and staging analyses.

Regional Aβ Quantification

Regional Aβ burden was quantified using continuous SUVR values extracted from cohort-specific parcellations: the Automated Anatomical Labeling (AAL) atlas[34] for SILCODE (yielding 60 cortical regions, *Supplementary Table S1*) and the Desikan–Killiany (DK) atlas[35] for HABS (yielding 52 cortical regions, *Supplementary Table S1*). Values from homologous left and right regions were averaged to obtain bilateral regional measures.

MRI Acquisition, Preprocessing and Network Analysis

Multimodal MRI data were available for all SILCODE participants, including high-resolution T1-weighted images, resting-state fMRI (rs-fMRI), and diffusion tensor imaging (DTI), acquired on a 3T GE Signa PET/MR scanner. Full acquisition parameters for each modality are provided in the *Supplementary Methods*.

Preprocessing followed a standardized pipeline[23]. T1-weighted images were segmented and normalized to MNI space. rs-fMRI preprocessing included removal of the first 5 volumes, motion and slice-timing correction, co-registration to T1, normalization using DARTEL, spatial smoothing, nuisance regression (Friston-24 motion parameters[36], white-matter and CSF signals), and temporal band-pass filtering. DTI preprocessing included motion and eddy-current correction, tensor fitting, and nonlinear registration to MNI space. Individual AAL masks were warped into native DTI space for tractography[37]. Detailed preprocessing pipelines for rs-fMRI and DTI are provided in the *Supplementary Methods*.

Functional and structural brain networks were constructed using AAL cortical regions as nodes. Functional connectivity matrices were generated by computing pairwise Pearson correlations between regional BOLD time series (correlation coefficient threshold of $r \geq 0.23$ in the main analysis). Structural connectivity matrices were derived using deterministic whole-brain tractography implemented in PANDA, and the weighted edge of a node pair was obtained by the number of fiber bundles connecting them (fiber-count threshold larger than 8 in the main analysis)[38,39].

Regional network topology of the functional and structural networks was quantified using three complementary regional centrality metrics: degree centrality, reflecting direct connection; betweenness centrality, reflecting a node's role in mediating communication across the network; and shortest path length, reflecting nodal accessibility and network efficiency (see *Supplementary Methods*), each averaged across hemispheres to obtain bilateral measures[40]. Network hubs were defined as regions exhibiting either degree centrality or betweenness centrality greater than one standard deviation above the network mean.

Reproducibility across network thresholds (four correlation thresholds range r = 0.13–0.43 with internal steps of 0.1 in the functional network and four fiber-count thresholds ranging from 3–18 with internal steps of 5 in the structural network) was confirmed. Detailed network construction and preprocessing procedures are provided in the *Supplementary Methods*.

Statistical Analyses

All statistical analyses were performed in MATLAB 2022a.

Baseline Cross-sectional Analyses in SILCODE

We examined whether regional Aβ burden and regional network topology jointly influenced baseline cognition. For each bilateral cortical region (*Supplementary Table S1*), three sequential general linear models were fitted:

$$model\,1:\ PACC\ \sim\ \beta_0 + \beta_1 \times A\beta_{regional} + Covs$$

$$model\,2:\ PACC\ \sim\ \beta_0 + \beta_1 \times A\beta_{regional} + \beta_2 \times Topo_{regional} + Covs$$

$$model\,3:\ PACC\ \sim\ \beta_0 + \beta_1 \times A\beta_{regional} + \beta_2 \times Topo_{regional} + \beta_3 \times \left(A\beta_{regional} \times Topo_{regional}\right) + Covs$$

All models were adjusted for age, sex, education, APOE ε4 status, baseline global SUVR, and site. False discovery rate (FDR) correction was applied across regions ($p < 0.05$).

For regions exhibiting a significant Aβ × topology interaction in Model 3, we further probed the conditional effect of regional topology on PACC across the observed range of regional Aβ using the Johnson–Neyman (J-N) technique[41], which identifies the values of the moderator (regional Aβ) at which the simple slope of regional topology becomes statistically significant, without imposing an arbitrary categorical cut-off point.

Regions showing significant main effect or interaction effects were carried forward for further characterization and validation.

Longitudinal Analyses in SILCODE: Within-cohort Validation

To test whether baseline regional Aβ burden or the baseline Aβ × topology interaction predicted future cognitive changes, we used linear mixed-effects (LME) models with random intercepts:

$$model\,4: Y_{it}\ \sim\ \beta_0 + \beta_1 \times A\beta_{regional} + \beta_2 \times Topo_{regional} + \beta_3 \times Time + \beta_4 \times \left(Time \times Topo_{regional}\right) + \beta_5 \times \left(Time \times A\beta_{region}\right.$$

Here, participants contributed variable numbers of follow-up visits over different durations (range 6-110 months), all available longitudinal observations were modeled jointly within a single mixed-effects framework, where Y_{it} represents the PACC score for participant i at time t. Covariates were age, sex, education, APOE ε4 status, scanning site and baseline global SUVR. Statistical significance was assessed at $p < 0.01$.

External Validation in Longitudinal HABS cohort data

To test whether baseline regional Aβ burden predicted future cognitive and amyloid changes at 3-year and 8-year follow-up, respectively, we used linear mixed-effects (LME) models with random intercepts:

$$model\,5: Y_{it}\ \sim\ \beta_0 + \beta_1 \times Time_{it} + \beta_2 \times A\beta_{regional,i} + \beta_3 \times \left(Time_{it} \times A\beta_{regional,i}\right) + Covs + (1|Subject)$$

where Y_{it} represents the continuous longitudinal outcome (PACC score or global SUVR) for participant i at time t. Covariates were age, sex, education, APOE ε4 status, scanning site and baseline global SUVR.

Statistical significance was assessed at FDR corrected levels ($p < 0.05$) to comprehensively evaluate the longitudinal replication strength of cross-sectionally derived regions from the SILCODE cohort.

Results

Cohort Characteristics

To capture the earliest chronological changes of Aβ pathology prior to widespread cortical accumulation, our study sample was restricted exclusively to individuals classified as gAβ- at their baseline assessment. The final analytical sample consisted of two independent cohorts: 73 gAβ- participants at baseline and 69 with follow-up ranging from 6 to 110 months in SILCODE, 157 gAβ- participants at baseline with 3-years and among them, 72 with 8-year follow-up in HABS. For detailed demographic and clinical characterizations see Table 1.

SILCODE: Structural Network Topology Modulates the Impact of Regional Aβ on Cross-sectional Cognition

We evaluated whether regional Aβ load impairs cross-sectional cognitive performance (PACC) and whether this relationship is modulated by nodal topology, using sequential linear regressions (Models 1–3) in each region (see *Supplementary Table S1*) across three nodal centrality metrics (degree, betweenness, and shortest path length) and four network density thresholds, adjusting for age, sex, education, APOE ε4 status, baseline global SUVR, and site.

Across Models 1 and 2, precuneus (PCUN; hereafter, the amyloid-dominant region) regional Aβ load demonstrated a significant main effect on cognition that was highly robust (all $P_{FDR} < 0.05$, Fig. 2A, Table 2; *Supplementary Table S2 and S3*). PCUN regional Aβ showed a robust association with cognition, surviving adjustment for global amyloid burden and extending to cognitive subtests (Fig. 2B).

Table 2
Significant effects of regional Aβ burden and its interaction effects with degree centrality on cognition in SILCODE.

Models	Effect	Regions	β	SE	T	Hubs
Model 1	Aβ main effect	PCUN	1.689	0.609	2.774 *	SN-hub
Model 3 (In the SN)	$\mathrm{A}\beta \times Dreg$ interaction effect	ACG	-0.007	0.003	-2.861 *	FN-hub
		IFGtriang	-0.007	0.002	-2.976 *	non
		SMG	-0.005	0.002	-2.895 *	FN-hub
		PHG	-0.009	0.003	-3.142 *	FN-hub
		STG	-0.003	< 0.001	-3.415 *	FN/SN-hub
		MTG	-0.003	< 0.001	-3.520 *	FN/SN-hub
		PoCG	-0.007	0.002	-2.980 *	non
	$\mathrm{A}\beta \times Lreg$ interaction effect	STG	-0.003	0.001	-3.413 *	FN/SN-hub
		MTG	-0.003	0.001	-3.573 *	FN/SN-hub
Model 3	$\mathrm{A}\beta \times Lreg \times \mathrm{Modality}$ interaction effect	STG	-46.250	14.409	-3.210 *	FN/SN-hub
		MTG	-38.435	11.823	-3.251 *	FN/SN-hub
Model 4	$\mathrm{A}\beta \times Dreg \times \mathrm{Time}$ interaction effect	ACG	-0.003	0.001	-2.637 *	FN-hub

Note: Values represent the regression coefficients (β), standard errors (SE), and t-values, where * represents FDR-corrected p < 0.05. PCUN, Precuneus; IFGtriang, Inferior frontal gyrus, triangle part; ACG, Anterior cingulate and paracingulate gyri; PHG, Para-hippocampal gyrus; PoCG, postcentral gyrus; SMG, supramarginal gyrus; STG, Superior temporal gyrus; MTG, Middle temporal gyrus; FN-hub, hub region in the functional network; SN-hub, hub region in the structural networks.

In Model 3, significant Aβ × topology interactions were observed predominantly within the structural network, confined to degree centrality and nodal shortest path length (all P_{FDR} < 0.05, Table 2 and *Supplementary Table S3*). Seven regions including the anterior cingulate gyrus (ACG), triangular part of the inferior frontal gyrus (IFGtriang), parahippocampal gyrus (PHG), supramarginal gyrus (SMG), postcentral gyrus (PoCG), superior temporal gyrus (STG), and middle temporal gyrus (MTG), hereafter referred to as network-dependent regions, demonstrated significant interaction effects for degree centrality (Fig. 3A and *Supplementary Figure S1A*) across all thresholds. Among them, STG and MTG also exhibited significant interaction effects for shortest path length, stable across all four structural network thresholds (Fig. 3B). The degree centrality of inferior parietal lobule (IPL) (*Supplementary Figure S1A*) and shortest path length of PoCG and IPL (*Supplementary Figure S1B*) showed similar interaction patterns but did not reach significance at all thresholds (*Supplementary Table S3*).

Post-hoc probing of the significant interaction effects using the Johnson–Neyman (J-N) approach revealed a consistent burden-dependent reversal of topology effects across network-vulnerable regions. Higher degree centrality and lower shortest path length were associated with better cognition at relatively lower regional Aβ burden, whereas these associations became negative after the conditional slope crossed zero at higher Aβ levels (Fig. 3A and 3B).

SILCODE: Baseline regional Aβ × topology interaction predicts longitudinal cognitive trajectories

In model 4, only a significant time × regional Aβ × regional degree of ACG interactions (β = -0.0002, p = 0.008; Fig. 4) was found. Post hoc analysis showed higher regional Aβ in the ACG combined with greater degree centrality in the ACG predicts accelerated cognitive decline over time.

SILCODE: Robustness and Topological Characterization

Overlap with network hub architecture - Regions showing significant main or interaction effects overlapped substantially with network hubs identified from the topological analyses (*Supplementary Figure S2 A&C*). In the functional network, SMG, STG, and MTG were betweenness hubs and PHG and ACG were degree hub. In the structural network, PCUN, STG, MTG, were betweenness hubs and degree hubs.

Modality-Specific Aβ–Topology Interactions - To determine whether the regional Aβ–topology interactions differed between structural and functional modalities, we tested a three-way interaction model including regional Aβ, nodal topology, and modality (structural v.s. functional). This analysis was restricted to the loosest network threshold and to those regions that showed significant Aβ × topology interactions effects in Model 3. Across all tested regions, the three-way interaction term (Aβ × topology × modality) was not statistically significant in degree centrality (all p > 0.05), but in shortest path length

of STG (β = -46.25, p = 0.002), MTG (β = -38.43, p = 0.002) (Fig. 3C), indicating that the moderating effect of nodal shortest path length on the Aβ and PACC association differ between structural and functional modalities.

HABS (3-years and 8-years follow-up): Baseline regional Aβ burden carries prognostic value for short and long-term cognitive and amyloid trajectories

Over 3 years, significant baseline regional Aβ × time interactions survived in the rACG (P_{FDR} < 0.05, Table 3, Fig. 5A), driven by an increase in PACC among participants with lower baseline Aβ burden. Baseline Aβ burden in the PCUN significantly predicted subsequent global amyloid accumulation over the 3-year follow-up period (P_{FDR} < 0.05, Table 3, Fig. 5B).

Table 3
Prediction of longitudinal changes of PACC and global amyloid accumulation.

Cohorts	Regions	Time × Regional Aβ interaction effects On PACC changes			Time × Regional Aβ interaction effects On global amyloid changes		
		β	SE	T	β	SE	T
HABS (0-3yrs)	rACG	-1.369	0.497	-2.752 *	/	/	/
	PCUN	/	/	/	0.378	0.113	3.349 *
HABS (0-8yrs)	rACG	-2.256	0.835	-2.701 *	/	/	/
	IFGtriang	-2.775	1.031	-2.692 *	/	/	/
	STG	-3.647	1.298	-2.810 *	/	/	/
	SMG	-2.825	0.989	-2.857 *	/	/	/
	PCUN	/	/	/	0.730	0.252	2.901 *

Across the 8-year follow-up period, significant baseline regional Aβ × time interactions survived in the IFGtriang, rACG, STG and SMG (P_{FDR} < 0.05, Table 3, Fig. 5C), showing that higher baseline amyloid burden within these regions was associated with worse long-term cognitive trajectories. Baseline Aβ burden in the precuneus (PCUN) significantly predicted subsequent global amyloid accumulation over the 8-year follow-up period (P_{FDR} < 0.05, Table 3, Fig. 5D).

Discussion

In this study, we investigated how early regional Aβ deposition in amyloid PET imaging relates to cognition before global amyloid positivity, and how this relationship is moderated by the structural and functional topological organization of the brain network. Across independent gAβ − cohorts, we identified two complementary pathways linking early amyloid pathology to cognition. First, regional Aβ burden in the precuneus emerged as a robust, topology-independent association with concurrent cognition, with higher regional Aβ associated with better cognitive performance in this early, globally amyloid-negative population. Second, in a distinct set of cortical regions occupying central positions within structural networks, the association of regional Aβ with concurrent cognition depended on local network topology. Higher structural centrality was associated with better cognition at relatively lower amyloid burden, whereas this association was reversed at higher amyloid levels, indicating that the cognitive impact of network organization varies as a function of regional amyloid burden. This topology-dependent framework received longitudinal support within SILCODE, where the regional Aβ × degree centrality interaction in the anterior cingulate gyrus predicted subsequent cognitive trajectories. Independent longitudinal validation in HABS cohorts further demonstrated the prognostic relevance of regional amyloid deposition, with baseline Aβ burden in several of the topology-dependent cortical regions predicting future cognitive changes. Finally, precuneus Aβ consistently predicted subsequent global amyloid accumulation. Together, these findings support a dual-route model of early amyloid-related cognitive vulnerability, in which an amyloid-dominant pathway centered on the precuneus and a network-dependent pathway shaped by local topology jointly determine the cognitive impact of early amyloid accumulation.

Our findings extend the conventional amyloid-centric view by demonstrating that the cognitive consequences of early Aβ deposition are not solely determined by regional amyloid burden[42–44], but critically depend on the topological position (hubs) of the affected region within the brain network[17,19,45]. Previous studies have established that Alzheimer's disease preferentially affects highly connected hub regions, which exhibit increased metabolic demands and serve as integrative center vulnerable to network disruption[46,47]. Such regions may amplify the impact of localized pathological insults because their extensive connectivity enables both efficient information integration and widespread propagation of dysfunction across distributed systems[20,44,45]. Consistent with this framework, we identified a distributed set of hub-associated cortical regions, including the ACG, temporal, frontal, and parietal regions, in which the cognitive relevance of regional Aβ burden depended on local structural network organization.

Our results refine this vulnerability framework by showing that network centrality is not uniformly detrimental but represents a dynamic property with context-dependent consequences. At relatively lower regional Aβ burden, greater structural centrality was associated with better cognition, potentially reflecting enhanced network efficiency, redundancy, and compensatory capacity[48]. However, once amyloid burden exceeded the transition range identified by Johnson–Neyman analyses, the same highly connected regions became associated with poorer cognition, suggesting a shift from network-related resilience to vulnerability[49]. The preferential expression of these effects in structural rather than functional networks further indicates that anatomical network organization provides the essential scaffold constraining the propagation of early pathology[50,51] that ultimately dictates down-stream cognitive consequences. This structural specificity aligns with recent evidence showing that incorporating individualized structural connectome, but not functional connectome, information into Aβ measures enhances prediction of future cognitive decline[27]. These findings suggest that network topology determines not

simply where amyloid accumulates as suggested by traditional cascade models[52,53], but fundamentally dictates when and how regional amyloid burden becomes cognitively consequential[27,49].

Among these topology-dependent regions, the anterior cingulate cortex provides the strongest longitudinal support for this topology-dependent mechanism. The ACG is a central component of large-scale cognitive control and salience networks, supporting adaptive regulation of distributed brain systems and maintaining flexible information processing[54]. Notably, our previous studies identified early network alterations involving the ACG at the early stage. In individuals with subjective cognitive decline, we observed increased functional connectivity of the ACG within limbic-related networks across independent Chinese and German cohorts[55], suggesting early functional reorganization that may reflect compensatory adaptation. The present study included a larger sample, with partial overlap with the Chinese cohort. Furthermore, graph-theoretical analyses demonstrated increased functional and structural network properties involving the ACG during subjective cognitive decline, with these topological alterations showing associations with amyloid stages[23]. In this study, the baseline regional Aβ × degree centrality interaction in the ACG predicted subsequent cognitive trajectories within SILCODE, and ACG Aβ burden alone showed prognostic value for future cognitive decline in independent HABS cohorts. These convergent findings suggest that the ACG represents a prototypical network-vulnerable region in which amyloid burden becomes cognitively meaningful only when considered within the context of its topological role.

The precuneus represents a biologically distinct pathway linking early amyloid pathology to cognition and disease progression. As one of the earliest and most consistently affected regions in AD, the precuneus shows preferential amyloid accumulation before widespread cortical involvement and clinical manifestation[11,13,56]. In contrast to the topology-dependent effects observed in other hub associated regions, precuneus Aβ exhibited a robust topology-independent positive association with concurrent cognition. Importantly, this association remained significant after adjustment for global amyloid burden, despite the strong relationship between regional and global amyloid measures, indicating that precuneus-specific deposition carries biological information at the earliest stages of amyloid accumulation and provides information beyond overall amyloid load. The positive direction of this association is counterintuitive and should therefore be interpreted cautiously within the restricted early disease window represented by globally amyloid-negative individuals. It should not be interpreted as evidence of a beneficial effect of amyloid pathology. One possible explanation is that this association is confounded by individual differences in cognitive reserve: individuals with greater reserve may tolerate, or take longer to accumulate, higher levels of regional Aβ before cognitive decline becomes apparent, while reserve itself independently supports better cognitive performance[57,58]. Under this account, reserve acts as a common cause of both higher regional Aβ and better cognition, rather than amyloid pathology itself conferring a cognitive benefit. However, the mechanisms underlying this positive association cannot be determined from the present cross-sectional data, and longitudinal designs capable of disentangling reserve, amyloid accumulation, and cognitive trajectories will be needed to test this possibility directly. Beyond cross-sectional cognition, the reproducible association between baseline precuneus Aβ and subsequent global amyloid accumulation across HABS cohorts supports the interpretation of precuneus deposition as an early staging marker. Previous frameworks have demonstrated that in vivo anatomical staging of amyloid deposition typically initiates within core default mode hubs[12], and longitudinal data confirm that this localized accumulation consistently precedes full-scale global positivity[13]. Together, these findings suggest that the precuneus serves as an amyloid-dominant region, where local pathology burden reflects an individual's position along the trajectory toward widespread amyloid accumulation.

Longitudinal analyses further clarify the temporal relationship between early regional amyloid pathology and subsequent cognitive change, and this relationship took a distinct form in each cohort and follow-up window. Within SILCODE, individuals with high baseline ACG amyloid burden and high degree centrality showed accelerated cognitive decline over follow-up (6-110 months), although a general negative trend was also present across other sub-groups, consistent with expected age-related decline superimposed on this pathology-specific effect. In the HABS 3-year follow-up, cognitive performance improved over time among individuals with low baseline ACC amyloid burden, whereas no such improvement was observed among those with high baseline ACC amyloid burden. This pattern is compatible with practice-related improvement commonly observed with repeated cognitive assessments in clinically normal older adults[59,60], one interpretation is that early regional pathology may blunt or offset an expected practice-related gain before producing measurable absolute decline. the HABS 8-year follow-up, by contrast, revealed a clearer relationship between baseline regional amyloid burden and subsequent cognitive decline. By contrast, over the 8-year follow-up, individuals with higher baseline Aβ deposition in several hub-associated regions, including IFGtriang, rACG, STG, and SMG, exhibited greater longitudinal cognitive deterioration. This longer observation window revealed a more consistent relationship between baseline regional amyloid burden and subsequent cognitive deterioration, suggesting that the prognostic relevance of early regional amyloid may become more apparent as disease-related changes accumulate over time.

Several limitations should be acknowledged. First, although the multi-cohort design and longitudinal analyses provide convergent evidence, the observational nature of this study precludes causal inference regarding whether regional Aβ accumulation drives network vulnerability or whether pre-existing network characteristics modulate the impact of amyloid pathology. Incorporating tau PET in future work will be important for clarifying how Aβ, tau, and network topology jointly shape early disease progression. Second, our analysis primarily relied on baseline network metrics to define regional vulnerability. However, brain network topology is dynamic and may undergo remodeling as pathology accumulates. The inclusion of longitudinal neuroimaging in future studies could better elucidate the reciprocal relationship between advancing pathology and the evolving network architecture. Third, although independent cohorts with different follow-up intervals were included, the relatively limited duration of some follow-up periods and the slow cognitive progression in globally amyloid-negative individuals constrain the detection of later clinical transitions. Longer prospective studies spanning the preclinical-to-symptomatic stages of AD will be needed to further establish the long-term clinical relevance of topology-dependent amyloid vulnerability.

Conclusion

In conclusion, our findings demonstrate that early regional Aβ deposition influences cognition through two complementary pathways before global amyloid positivity. Longitudinal observations further support the prognostic relevance of these mechanisms. Together, these findings extend amyloid-centric models

by demonstrating that the clinical significance of early Aβ pathology depends not only on the amount of amyloid accumulated, but also on where and how pathology interacts within the brain's network architecture.

Data availability

Data in the HABS are provided in the HABS resources (https://habs.mgh.harvard.edu/). Data in the SILCODE that support the findings of this study are available from the corresponding author (Dr. Y. Han), upon reasonable request.

Declarations

Contributions

Study concept and design: Dr. C. Yan and Dr. X. Jiang. Data analysis and interpretation: Dr. X. Jiang and Dr. C. Yan. Writing manuscript: Dr. X. Jiang and Dr. C. Yan. Critical revision of the manuscript: Dr. X. Jiang, Dr. H. Boecker, Dr. M. Daamen and Dr. X. Hu. Final check: Dr. C. Yan, Dr. H. Boecker, Dr. M. Daamen, Dr. X. Hu, Dr. H. Wang, Dr. Y. Han and Dr. X. Jiang.

Competing interests

The authors report no Conflicts of Interest relevant to the manuscript.

Note

Values represent fixed-effect estimates from linear mixed-effects models (Model 5) evaluating whether baseline regional Aβ burden predicts longitudinal PACC change. Columns show regression coefficients (β), standard errors (SE), and t-values for the Time effect, baseline regional Aβ effect, and the Time × regional Aβ interaction. Significance markers reflect p-values (FDR corrected $p < 0.05$ (*)). IFGtriang, Inferior frontal gyrus, triangle part; rACG, rostral anterior cingulate; PCUN, Precuneus; SMG, supramarginal gyrus; STG, Superior temporal gyrus.

Author Contribution

Study concept and design: Dr. C. Yan and Dr. X. Jiang. Data analysis and interpretation: Dr. X. Jiang and Dr. C. Yan. Writing manuscript: Dr. X. Jiang and Dr. C. Yan. Critical revision of the manuscript: Dr. X. Jiang, Dr. H. Boecker, Dr. M. Daamen and Dr. X. Hu. Final check: Dr. C. Yan, Dr. H. Boecker, Dr. M. Daamen, Dr. X. Hu, Dr. H. Wang, Dr. Y. Han and Dr. X. Jiang.

Acknowledgements

The authors thank the patients for their participation in this research. This article was supported by NSFC (82603978, 82327809, 82020108013, 62303143, 32300864), Qiantang Scholars Program, Tianchi Scholars Program, the Hainan Provincial Natural Science Foundation of China (No. 825QN286), the China Postdoctoral Science Foundation under Grant Number 2025M773452 and Jiangsu Funding Program for Excellent Postdoctoral Talent. AI tools, including ChatGPT 4.0 (OpenAI) and DeepSeek, were used to refine, edit, and format portions of the manuscript. The authors take full responsibility for the content and accuracy of the manuscript.

Datasets reported in this publication was also supported by the National Institute on Aging of the National Institutes of Health under Award Numbers R01AG054073, R01AG058533, R01AG070862, P41EB015922 and U19AG078109. The content is solely the responsibility of the authors and does not necessarily represent the official views of the National Institutes of Health.

Data Availability

Data in the HABS are provided in the HABS resources (https://habs.mgh.harvard.edu/). Data in the SILCODE that support the findings of this study are available from the corresponding author (Dr. Y. Han), upon reasonable request.

References

1. Hampel H, et al. The Amyloid-β Pathway in Alzheimer's Disease. Mol Psychiatry. 2021;26:5481–503.
2. Sperling RA, et al. Toward defining the preclinical stages of Alzheimer's disease: Recommendations from the National Institute on Aging-Alzheimer's Association workgroups on diagnostic guidelines for Alzheimer's disease. Alzheimer's Dement : J Alzheimer's Association. 2011;7:280.
3. Sims JR, et al. Donanemab in Early Symptomatic Alzheimer Disease. JAMA. 2023;330:512–27.
4. Van Dyck CH, et al. Lecanemab in Early Alzheimer's Disease. N Engl J Med. 2023;388:9–21.
5. Dubois B, et al. Preclinical Alzheimer's disease: Definition, natural history, and diagnostic criteria. Alzheimers Dement. 2016;12:292–323.

6. Jack CR Jr, et al. Revised criteria for diagnosis and staging of Alzheimer's disease: Alzheimer's Association Workgroup. Alzheimer's Dement. 2024;20:5143–69.
7. Jack CR, et al. Update on hypothetical model of Alzheimer's disease biomarkers. Lancet Neurol. 2013;12:207–16.
8. Klunk WE, et al. The Centiloid Project: Standardizing Quantitative Amyloid Plaque Estimation by PET. Alzheimers Dement. 2015;11:1–e154.
9. Cui L, et al. Beyond binary classification: Comparing three region-based multi-phase Aβ staging systems. Alzheimers Dement. 2025;21:e70253.
10. Insel PS, Donohue MC, Sperling R, Hansson O. Mattsson-Carlgren, N. The A4 study: β-amyloid and cognition in 4432 cognitively unimpaired adults. Ann Clin Transl Neurol. 2020;7:776–85.
11. Buckner RL, et al. Molecular, Structural, and Functional Characterization of Alzheimer's Disease: Evidence for a Relationship between Default Activity, Amyloid, and Memory. J Neurosci. 2005;25:7709–17.
12. Grothe MJ, et al. In vivo staging of regional amyloid deposition. Neurology. 2017;89:2031–8.
13. Palmqvist S, et al. Earliest accumulation of β-amyloid occurs within the default-mode network and concurrently affects brain connectivity. Nat Commun. 2017;8:1214.
14. Alchera N, et al. Patterns of amyloid accumulation in amyloid-negative cases. Neurobiol Aging. 2023;129:99–108.
15. Farrell ME et al. Regional amyloid accumulation and cognitive decline in initially amyloid-negative adults. Neurology 91, (2018).
16. Hedden T, Oh H, Younger AP, Patel TA. Meta-analysis of amyloid-cognition relations in cognitively normal older adults. Neurology. 2013;80:1341–8.
17. Buckner RL, et al. Cortical Hubs Revealed by Intrinsic Functional Connectivity: Mapping, Assessment of Stability, and Relation to Alzheimer's Disease. J Neurosci. 2009;29:1860–73.
18. van den Heuvel MP, Sporns O. Network hubs in the human brain. Trends Cogn Sci. 2013;17:683–96.
19. Crossley NA, et al. The hubs of the human connectome are generally implicated in the anatomy of brain disorders. Brain. 2014;137:2382–95.
20. Jin S, Wang J, He Y. The brain network hub degeneration in Alzheimer's disease. Biophys Rep. 2024;10:213–29.
21. Liu G, Shen C, Qiu A. Amyloid-β accumulation in relation to functional connectivity in aging: A longitudinal study. NeuroImage. 2023;275:120146.
22. Drzezga A, et al. Neuronal dysfunction and disconnection of cortical hubs in non-demented subjects with elevated amyloid burden. Brain. 2011;134:1635–46.
23. Jiang X et al. Brain Topological Changes in Subjective Cognitive Decline and Associations with Amyloid Stages. Preprint at https://doi.org/10.21203/rs.3.rs-4459273/v1 (2025).
24. Han F, Liu X, Mailman RB, Huang X, Liu X. Resting-state global brain activity affects early β-amyloid accumulation in default mode network. Nat Commun. 2023;14:7788.
25. Moffat G, Zhukovsky P, Coughlan G, Voineskos AN. Unravelling the relationship between amyloid accumulation and brain network function in normal aging and very mild cognitive decline: a longitudinal analysis. Brain Commun. 2022;4:fcac282.
26. Sepulcre J, et al. Tau and amyloid β proteins distinctively associate to functional network changes in the aging brain. Alzheimer's Dement. 2017;13:1261–9.
27. He H, Razlighi QR, Gazes Y, Habeck C, Stern Y. Integrating individualized connectome with amyloid pathology improves predictive modeling of future cognitive decline. Commun Med. 2025;5:515.
28. Li X, Wang X, Su L, Hu X, Han Y. Sino Longitudinal Study on Cognitive Decline (SILCODE): protocol for a Chinese longitudinal observational study to develop risk prediction models of conversion to mild cognitive impairment in individuals with subjective cognitive decline. BMJ Open. 2019;9:e028188.
29. Dagley A, et al. Harvard Aging Brain Study: dataset and accessibility. NeuroImage. 2017;144:255–8.
30. Donohue MC, et al. The Preclinical Alzheimer Cognitive Composite. JAMA Neurol. 2014;71:961–70.
31. Katzman R, et al. A Chinese version of the mini-mental state examination; Impact of illiteracy in a Shanghai dementia survey. J Clin Epidemiol. 1988;41:971–8.
32. Landau SM, et al. Amyloid PET imaging in Alzheimer's disease: A comparison of three radiotracers. Eur J Nucl Med Mol Imaging. 2014;41:1398–407.
33. Gottesman RF, et al. Association between midlife vascular risk factors and estimated brain amyloid deposition. JAMA. 2017;317:1443–50.
34. Tzourio-Mazoyer N et al. Automated Anatomical Labeling of Activations in SPM Using a Macroscopic Anatomical Parcellation of the MNI MRI Single-Subject Brain. *NeuroImage* 15, 273–289 (2002).
35. Desikan RS, et al. An automated labeling system for subdividing the human cerebral cortex on MRI scans into gyral based regions of interest. NeuroImage. 2006;31:968–80.
36. Friston KJ, Williams S, Howard R, Frackowiak RSJ, Turner R. Movement-Related effects in fMRI time-series. Magn Reson Med. 1996;35:346–55.
37. Cui Z, Zhong S, Xu P, He Y, Gong G. PANDA: a pipeline toolbox for analyzing brain diffusion images. Front Hum Neurosci 7, (2013).
38. Gong G, et al. Mapping Anatomical Connectivity Patterns of Human Cerebral Cortex Using In Vivo Diffusion Tensor Imaging Tractography. Cereb Cortex. 2009;19:524–36.
39. Lo C-Y, et al. Diffusion Tensor Tractography Reveals Abnormal Topological Organization in Structural Cortical Networks in Alzheimer's Disease. J Neurosci. 2010;30:16876–85.
40. Bullmore E, Sporns O. Complex brain networks: graph theoretical analysis of structural and functional systems. Nat Rev Neurosci. 2009;10:186–98.
41. Bauer DJ, Curran PJ. Probing Interactions in Fixed and Multilevel Regression: Inferential and Graphical Techniques. Multivar Behav Res. 2005;40:373–400.

42. Hanseeuw BJ, et al. Association of Amyloid and Tau With Cognition in Preclinical Alzheimer Disease. JAMA Neurol. 2019;76:915–24.
43. Jack CR, et al. NIA-AA Research Framework: Toward a biological definition of Alzheimer's disease. Alzheimer's Dement. 2018;14:535–62.
44. Pini L, Allali G, Imbimbo BP, Germani M, Corbetta M. Brain connectivity as a new target for Alzheimer's disease therapy? Brain. 2026;149:432–8.
45. Gupta R. Network-centric perspectives on neurodegeneration: Mechanisms, biomarkers, and therapeutic pathways. Brain Netw Disorders. 2026;02:17–25.
46. Seeley WW, Crawford RK, Zhou J, Miller BL, Greicius MD. Neurodegenerative diseases target large-scale human brain networks. Neuron. 2009;62:42–52.
47. Yu M, Sporns O, Saykin AJ. The human connectome in Alzheimer disease — relationship to biomarkers and genetics. Nat Rev Neurol. 2021;17:545–63.
48. Qiu T, et al. Structural white matter properties and cognitive resilience to tau pathology. Alzheimer's Dement. 2024;20:3364–77.
49. Stam CJ. Hub overload and failure as a final common pathway in neurological brain network disorders. Netw Neurosci. 2024;8:1–23.
50. Ottoy J, et al. Tau follows principal axes of functional and structural brain organization in Alzheimer's disease. Nat Commun. 2024;15:5031.
51. Raj A, Kuceyeski A, Weiner MA. Network Diffusion Model of Disease Progression in Dementia. Neuron. 2012;73:1204–15.
52. Iturria-Medina Y, Sotero RC, Toussaint PJ, Evans AC. Initiative, and the A. D. N. Epidemic Spreading Model to Characterize Misfolded Proteins Propagation in Aging and Associated Neurodegenerative Disorders. PLoS Comput Biol. 2014;10:e1003956.
53. Jones DT, et al. Cascading network failure across the Alzheimer's disease spectrum. Brain. 2016;139:547–62.
54. Seeley WW, et al. Dissociable Intrinsic Connectivity Networks for Salience Processing and Executive Control. J Neurosci. 2007;27:2349–56.
55. Jiang X, et al. Altered limbic functional connectivity in individuals with subjective cognitive decline: Converging and diverging findings across Chinese and German cohorts. Alzheimer's Dement. 2023;19:4922–34.
56. Sperling RA, et al. Amyloid deposition is associated with impaired default network function in older persons without dementia. Neuron. 2009;63:178–88.
57. Barulli D, Stern Y. Efficiency, capacity, compensation, maintenance, plasticity: emerging concepts in cognitive reserve. Trends Cogn Sci. 2013;17. 10.1016/j.tics.2013.08.012.
58. Stern Y. What is cognitive reserve? Theory and research application of the reserve concept. J Int Neuropsychol Soc. 2002;8:448–60.
59. Mormino EC, et al. Synergistic Effect of β-Amyloid and Neurodegeneration on Cognitive Decline in Clinically Normal Individuals. JAMA Neurol. 2014;71:1379–85.
60. Papp KV, Rentz DM, Orlovsky I, Sperling RA, Mormino EC. Optimizing the preclinical Alzheimer's cognitive composite with semantic processing: The PACC5. Alzheimers Dement (N Y). 2017;3:668–77.

Figures

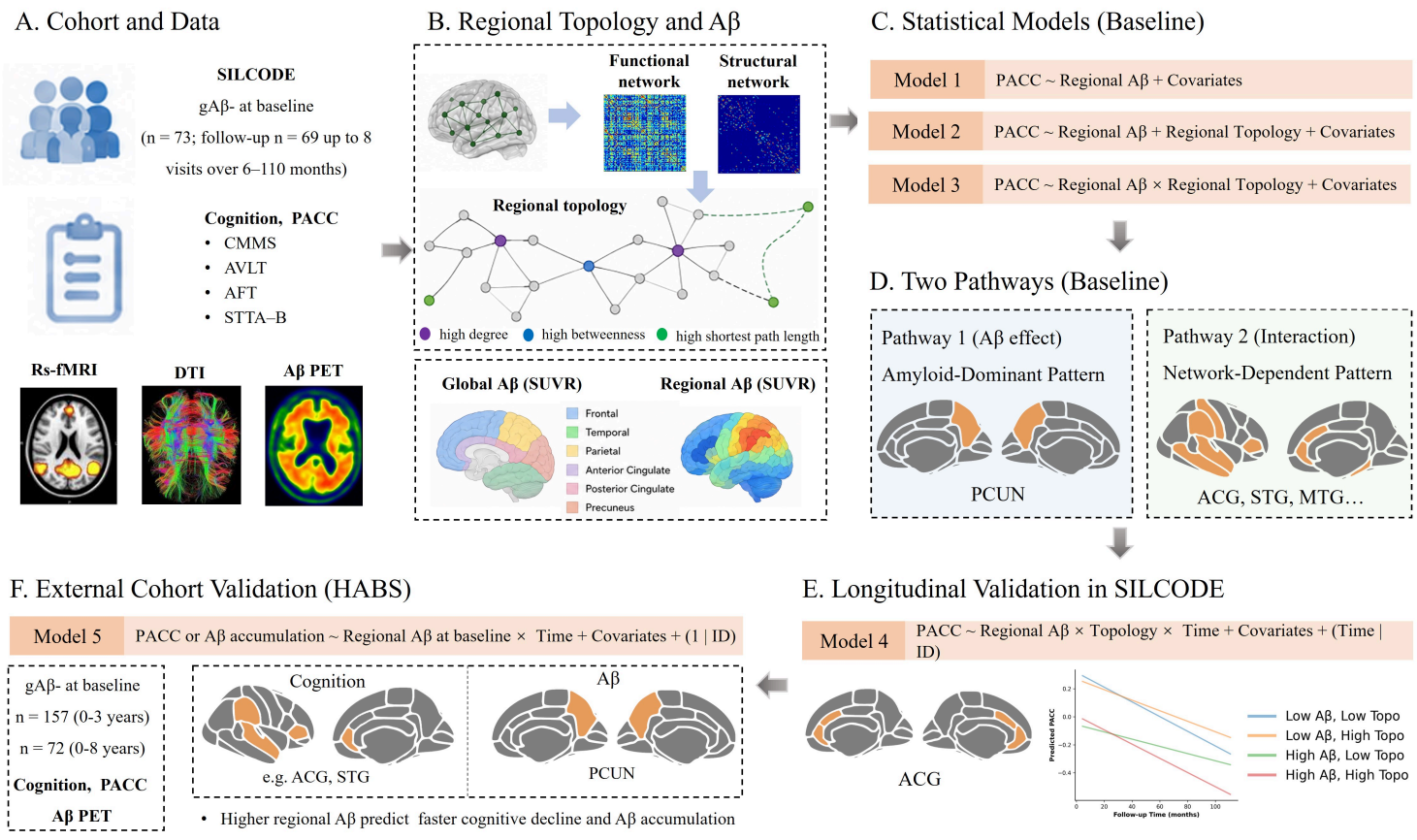


Figure 1

Study design and analytical framework. A) Cohort and data. Globally amyloid-negative (gAβ-) participants in SILCODE underwent cognitive assessment, rs-fMRI, DTI, and amyloid PET. B) Regional Aβ and network topology. Regional Aβ burden was quantified using continuous SUVRs, and regional topology was characterized in functional and structural networks using degree centrality, betweenness centrality, and shortest path length. C) Statistical models. Sequential baseline models tested the main effects and interaction between regional Aβ and network topology. D) Two pathways. Amyloid-dominant and network-dependent pathways linking early regional Aβ deposition to cognition before global amyloid positivity. E) Longitudinal validation in SILCODE. Model 4 examined longitudinal cognitive trajectories. F) External cohort validation in HABS. Model 5 examined longitudinal cognitive and amyloid trajectories across 3- and 8-year follow-up periods.

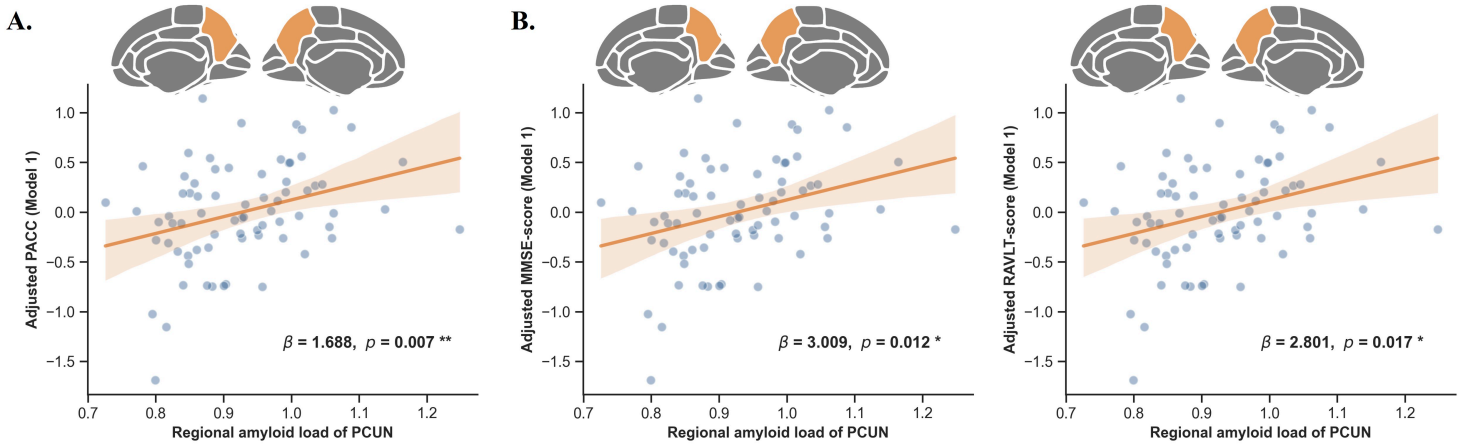


Figure 2

Association between precuneus amyloid burden and cognitive performance in globally amyloid-negative individuals. Scatter plot illustrating the positive association between regional PCUN Aβ burden and A) adjusted Preclinical Alzheimer Cognitive Composite (PACC) scores and B) adjusted Chinese-Mini-Mental State Examination (CMMSE) scores and Rey Auditory Verbal Learning Test (RAVLT) scores.

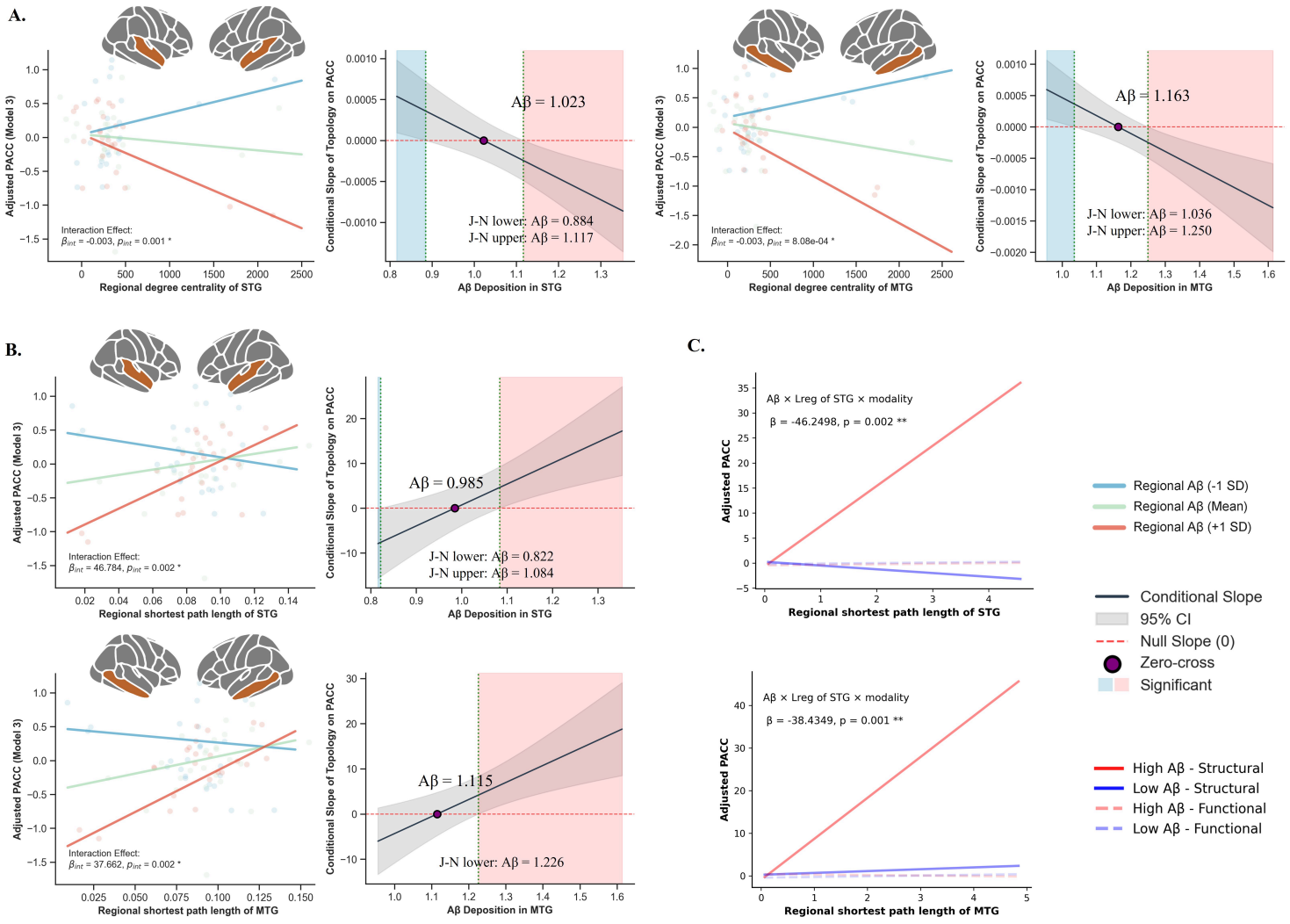


Figure 3

Regional topology moderates the association between regional Aβ burden and cognition and exhibits modality-specific effects. Regions showing significant regional Aβ and A) structural degree centrality, B) shortest path length interactions are presented, including the STG and MTG. Left panels show fitted interaction effects between regional Aβ burden and degree centrality, with conditional associations with PACC estimated at low (−1 SD), mean, and high (+1 SD) levels of amyloid burden. Right panels display Johnson–Neyman regions of significance, indicating the range of regional Aβ burden over which degree centrality was significantly associated with cognition. The crossover points demonstrate a transition from positive to negative associations between structural centrality and cognition with increasing regional Aβ burden. C) Three-way interaction analyses testing regional Aβ × shortest path length × network modality revealed significant modality-dependent effects in STG and MTG.

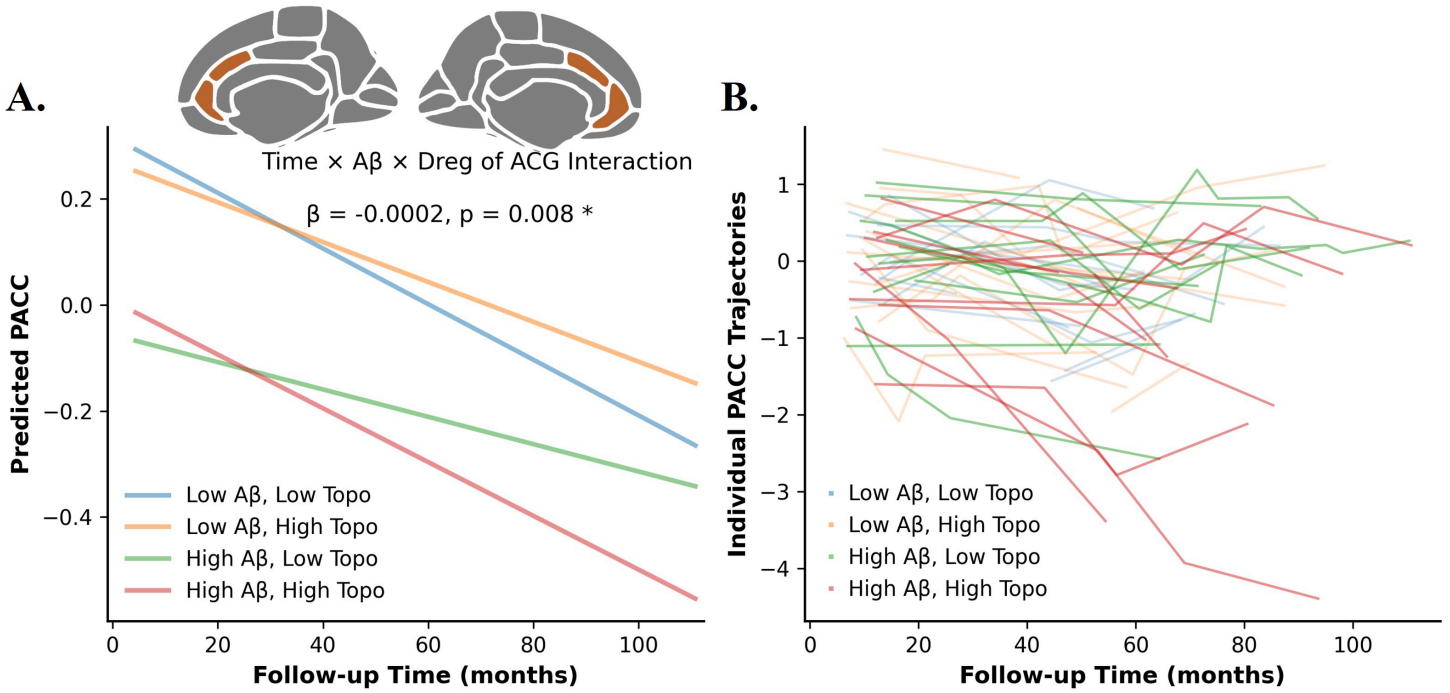


Figure 4

Baseline regional Aβ burden and structural degree centrality jointly predict longitudinal cognitive trajectories. A) significant Time × regional Aβ × degree centrality interaction shows estimated longitudinal PACC trajectories for the four combinations of baseline regional Aβ burden (low/high) and structural degree centrality (low/high) in the ACG; B) individual longitudinal PACC trajectories grouped according to baseline regional Aβ burden and degree centrality (low Aβ/low topology, low Aβ/high topology, high Aβ/low topology, and high Aβ/high topology).

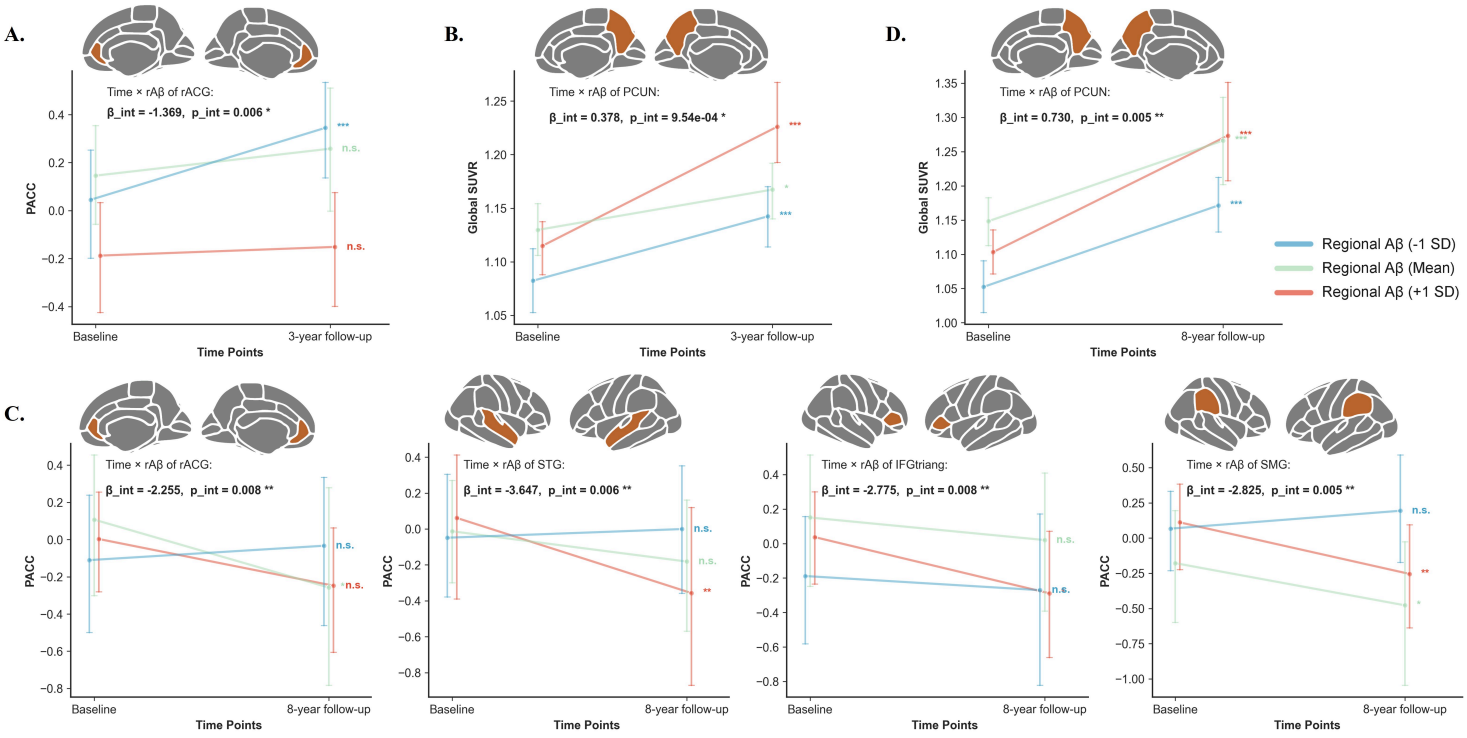


Figure 5

Longitudinal associations of baseline regional Aβ burden with subsequent cognitive trajectories and amyloid progression in HABS. Baseline regional Aβ burden was associated with A) 3-year follow-up and B) 8-year follow-up in HABS. Baseline precuneus Aβ burden consistently predicted longitudinal increases in global amyloid burden across C) HABS 3- year and D) 8-year follow-up periods.

Supplementary Files

This is a list of supplementary files associated with this preprint. Click to download.

- Table1.docx
- Table2.docx
- Table3.docx
- FinalSupplementaryMaterials.docx